

Associations between White Matter Hyperintensities and β Amyloid on Integrity of Projection, Association, and Limbic Fiber Tracts Measured with Diffusion Tensor MRI

Linda L. Chao^{1,2*}, Charles DeCarli³, Stephen Kriger², Diana Truran², Yu Zhang^{1,2}, Joel Laxamana², Sylvia Villeneuve⁴, William J. Jagust^{4,5}, Nerses Sanossian⁶, Wendy J. Mack⁷, Helena C. Chui⁶, Michael W. Weiner^{1,2}

1 Department of Radiology & Biomedical Imaging, University of California San Francisco, San Francisco, California, United States of America, **2** Center for Imaging of Neurodegenerative Diseases, Veterans Affairs Medical Center, San Francisco, San Francisco, California, United States of America, **3** Department of Neurology, University of California Davis, Davis, California, United States of America, **4** Helen Wills Neuroscience Institute, University of California, Berkeley, California, United States of America, **5** School of Public Health, University of California, Berkeley, California, United States of America, **6** Department of Neurology, University of Southern California, Los Angeles, California, United States of America, **7** Department of Preventive Medicine, University of Southern California, Los Angeles, California, United States of America

Abstract

The goal of this study was to assess the relationship between A β deposition and white matter pathology (i.e., white matter hyperintensities, WMH) on microstructural integrity of the white matter. Fifty-seven participants (mean age: 78 \pm 7 years) from an ongoing multi-site research program who spanned the spectrum of normal to mild cognitive impairment (Clinical dementia rating 0–0.5) and low to high risk factors for arteriosclerosis and WMH pathology (defined as WMH volume >0.5% total intracranial volume) were assessed with positron emission tomography (PET) with Pittsburgh compound B (PiB) and magnetic resonance and diffusion tensor imaging (DTI). Multivariate analysis of covariance were used to investigate the relationship between A β deposition and WMH pathology on fractional anisotropy (FA) from 9 tracts of interest (i.e., corona radiata, internal capsule, cingulum, parahippocampal white matter, corpus callosum, superior longitudinal, superior and inferior front-occipital fasciculi, and fornix). WMH pathology was associated with reduced FA in projection (i.e., internal capsule and corona radiata) and association (i.e., superior longitudinal, superior and inferior fronto-occipital fasciculi) fiber tracts. A β deposition (i.e., PiB positivity) was associated with reduced FA in the fornix and splenium of the corpus callosum. There were interactions between PiB and WMH pathology in the internal capsule and parahippocampal white matter, where A β deposition reduced FA more among subjects with WMH pathology than those without. However, accounting for apoE ϵ 4 genotype rendered these interactions insignificant. Although this finding suggests that apoE4 may increase amyloid deposition, both in the parenchyma (resulting in PiB positivity) and in blood vessels (resulting in amyloid angiopathy and WMH pathology), and that these two factors together may be associated with compromised white matter microstructural integrity in multiple brain regions, additional studies with a longitudinal design will be necessary to resolve this issue.

Citation: Chao LL, DeCarli C, Kriger S, Truran D, Zhang Y, et al. (2013) Associations between White Matter Hyperintensities and β Amyloid on Integrity of Projection, Association, and Limbic Fiber Tracts Measured with Diffusion Tensor MRI. PLoS ONE 8(6): e65175. doi:10.1371/journal.pone.0065175

Editor: Karl Herholz, University of Manchester, United Kingdom

Received: February 27, 2013; **Accepted:** April 23, 2013; **Published:** June 6, 2013

Copyright: © 2013 Chao et al. This is an open-access article distributed under the terms of the Creative Commons Attribution License, which permits unrestricted use, distribution, and reproduction in any medium, provided the original author and source are credited.

Funding: This work was supported by National Institutes of Health (NIH)/National Institute on Aging (NIA) PO1 AG012435, NIH/NIA P30AG010129 and the NIH/National Center for Research Resources P41RR023953, which were administered by the Northern California Institute for Research and Education, and with resources of the Veterans Affairs Medical Center, San Francisco, California. The funders had no role in study design, data collection and analysis, decision to publish, or preparation of the manuscript.

Competing Interests: LC is a PLOS ONE Editorial Board member. This does not alter the authors' adherence to all the PLOS ONE policies on sharing data and materials.

* E-mail: linda.chao@ucsf.edu

Introduction

Focal and diffuse lesions in the white matter, seen as hyperintensities on T2-weighted magnetic resonance images (MRI) (i.e., white matter hyperintensities; WMH) are the most ubiquitous age-related alteration seen in the brain [1]. From an etiological perspective, heterogeneity exists with respect to the presence of WMH. On one hand, they are related to cardiovascular risk factors, such as hypertension and atherosclerosis [2–4]. On the other hand, they are abundantly present in patients with an underlying amyloid pathology such as cerebral amyloid angiopathy (CAA) [5]. Another common pathological change in the aging brain is cerebral β -amyloid (A β) deposition. A β is the

major component of amyloid plaques and has been hypothesized to initiate a pathogenic cascade that eventually leads to Alzheimer's disease (AD) [6]. A β deposition and vascular brain injury frequently coexist [7,8]. We recently showed that aggregate coronary disease risk has a moderately strong association with cerebral amyloid deposition [9], consistent with the theory that vascular risk factors (e.g., low high density lipoprotein) contribute to AD pathology [10]. The goal of this study was to assess the relationship between A β deposition and WMH pathology, defined as greater than 0.5% of total intracranial volume (ICV) [11], on microstructural integrity of the white matter.

Diffusion tensor imaging (DTI) measures the organization of fibers within specific white matter tracts [12]. An indirect measure

of the coordinated directionality and coherence of fibers within a white matter fiber bundle [13], fractional anisotropy (FA) values typically decrease in the presence of pathology such as stroke [14] and WMH [15]. Here we used DTI to determine the regional pattern of FA disruption associated with WMH pathology and A β deposition. Based on previous DTI studies in patients with AD and mild cognitive impairment (MCI), a prodromal phase of AD, we hypothesized that A β deposition would be associated with decreased FA in the limbic circuit [16–20] (e.g., cingulum, parahippocampal white matter, and fornix) and posterior regions of the corpus callosum [21,22]. Because the anterior internal capsule and supratentorial white matter are common locations for WMH in the human brain [23], we hypothesized that WMH pathology would be associated with lower FA in projection (e.g., internal capsule and corona radiata) and association (e.g., superior longitudinal, superior and inferior fronto-occipital fasciculi) fiber tracts and in the corpus callosum, the major white matter structure involved in intrahemispheric cortico-cortical communication.

Recent epidemiologic studies have noted that risk factors for atherosclerosis (e.g., diabetes mellitus, hypertension, and hyperlipidemia) are also associated with increased risk of incident AD [24,25]. Moreover, it has been suggested that vascular brain injury may interact with concomitant AD pathology [26]. For this reason, we hypothesized that there would be an interaction between A β deposition and WMH pathology on FA. In particular, we looked for a A β deposition by WMH pathology interaction in the corpus callosum because Lee et al [27], previously reported differential region-specific associations between AD degenerative and vascular processes on the structural integrity of the corpus callosum.

Methods

Subjects

Subjects were older adults from the ongoing multi-site Aging Brain research program designed to recruit individuals with substantial risk factors for arteriosclerosis and vascular brain injury [9]. Persons with history of multiple vascular risk factors, coronary or carotid disease, myocardial infarction, or ischemic stroke were targeted for inclusion. Exclusion criteria included evidence of alcohol or substance abuse, head trauma with loss of consciousness lasting longer than 15 minutes, factors contraindicating MRI, and severe medical illness, neurologic or psychiatric disorders unrelated to AD or vascular dementia that could significantly affect brain structure (e.g., schizophrenia and other psychotic disorders, liver disease, multiple sclerosis, amyotrophic lateral sclerosis).

This study focused on a subset of 57 individuals who had PiB PET and DTI data. The mean time between acquisition of the PiB and DTI imaging data was 3.9 ± 4.9 months (range: 0–19 months). The subjects received clinical diagnostic evaluations at the Alzheimer's Disease Centers at the University of California at Davis and San Francisco. For purposes of analyses, the participants were classified by their Clinical Dementia Rating (CDR [28]) scores. Twenty-nine subjects (51%) had CDRs of 0 while 28 (49%) had CDRs of 0.5. Table 1 provides more details on participant characteristics.

Ethics Statement

The study was approved by the University of California (Davis, San Francisco, and Berkeley) and Lawrence Berkeley National Laboratory institutional review boards (IRB) for human research. Written informed consent was obtained from all participants or their legally authorized representatives following IRB-approved protocols. If there was an indication of cognitive impairment (e.g.,

in cases where the study participant had a CDR of 0.5 and/or a diagnosis of MCI), the study personnel obtaining consent would first assess whether or not the potential participant understood key elements of the protocol, including that participation is voluntary, that it is a research study, the procedures, the risks and benefits. If the potential participant lacked the capacity to provide informed consent, then informed consent was obtained from the participant's legally authorized representative in accordance with California law and the policy of the IRB of all participating institutions. The majority of participants with CDRs of 0.5 had the capacity to provide informed consent.

MRI Acquisition

MRI images were collected on Siemens 3 T MRI systems. Eight participants were scanned using a 3 T Siemens Magnetom Trio Syngo System with an 8-channel head coil at the University of California, Davis (UCD) research center. Acquired images included a T1-weighted volumetric MP-RAGE (TR = 2500, TE = 2.98, TI = 1100, $1 \times 1 \times 1$ mm³ isotropic resolution), a Fluid-Attenuated Inversion Recovery (FLAIR) scan (TR = 5000, TE = 430, TI = 1700 ms, with $1 \times 1 \times 2$ mm³ resolution), a T2-weighted turbo spin echo sequence for intracranial volume (ICV) determination (TR/TE: 3400/402 ms, $1 \times 1 \times 1$ mm³ isotropic resolution), and DTI scans obtained with a dual spin-echo EPI sequence, augmented by diffusion weighting gradients ($b = 800$ s/mm²) along six collinear directions and the acquisition of a reference image ($b = 0$). Other parameters of DTI were TR/TE = 10,000/101 ms, 60 slices $2 \times 2 \times 2$ mm³ resolution. Twofold parallel imaging acceleration was used for DTI to reduce geometrical distortions [29], and five scans were averaged to boost the signal.

Forty-three participants were scanned at UCD using a 3 T Siemens Magnetom TrioTim system with an 8-channel head coil. Six participants were scanned at the University of California, San Francisco (UCSF) Neuroscience Imaging Center using a 3 T Siemens Magnetom TrioTim system with a 12-channel head coil. Acquired images for the participants scanned on the 3 T Siemens Magnetom TrioTim system at UCD and UCSF included a T1-weighted volumetric MP-RAGE (TR = 2500, TE = 2.98, TI = 1100, $1 \times 1 \times 1$ mm³ isotropic resolution), a FLAIR scan (TR = 8800, TE = 495, TI = 2360 ms, with $1 \times 1 \times 2$ mm³ resolution), a T2-weighted turbo spin echo sequence (TR/TE: 3400/402 ms, $1 \times 1 \times 1$ mm³ isotropic resolution), and DTI scans obtained with a dual spin-echo EPI sequence supplemented with GRAPPA to reduce susceptibility distortions (TR/TE = 9000/101 ms, 60 slices $2 \times 2 \times 2$ mm³ resolution; 5 scans averaged to boost the signal).

Infarcts

Infarcts, identified by a vascular neurologist (NS) blind to any other participant data using the T1 and FLAIR MRIs, were identified on 22 of the 57 participants (39%). Infarcts were categorized according to affected vascular territory, structures involved, size (small 3–10 mm, large: >10 mm), severity (cystic, not cystic), and number. Table 2 presents a summary of the description of the participants' infarcts.

Apolipoprotein E Genotyping

Blood was drawn with the subject's consent for apolipoprotein E (apoE) genotyping, available for 48 of the 57 participants. Subjects with 3/4 or 4/4 combined alleles were classified as apoE $\epsilon 4$ positive, and those with 3/3 alleles as apoE $\epsilon 4$ negative. Because the 2/4 combined allele is associated with a lower risk of AD [30],

Table 1. Sample characteristics by PiB and WMH pathology^a status.

	PiB–	PiB+	WMH–	WMH+	PiB effect	WMH effect
	(N = 30)	(N = 27)	(N = 30)	(N = 27)	p-value	p-value
Age (yrs)	77.3 (7.3)	79.0 (6.6)	77.0 (7.0)	79.1 (6.9)	0.76 ^d	0.22 ^d
Sex (M/F)	20/10	20/7	23/7	17/10	0.54 ^e	0.26 ^e
Education (yrs)	14.3 (3.0)	14.7 (3.1)	14.6 (3.3)	14.4 (2.7)	0.67 ^d	0.84 ^d
MMSE	28.5 (2.0)	28.1 (2.0)	28.3 (2.0)	28.2 (2.0)	0.49 ^d	0.84 ^d
GDS	1.4 (1.8)	2.4 (2.7)	2.0 (2.6)	1.8 (1.9)	0.12 ^d	0.76 ^d
CDR 0/0.5	19/11	10/17	16/14	13/14	0.047 ^e	0.70 ^e
apoE ϵ 4 (–/+) ^b	21/5	13/9	19/7	15/7	0.10 ^e	0.71 ^e
Global PiB index	1.00 (0.00)	1.26 (0.45)	1.17 (0.38)	1.10 (0.27)	0.001 ^d	0.30 ^d
PiB –/+			16/14	14/13		0.91 ^e
Brain infarct on MRI	9 (30%)	13 (48%)	10 (33%)	12 (44%)	0.16 ^e	0.39 ^e
WMH ^c volume as % ICV	0.50 (0.64)	0.81 (0.89)	0.20 (0.12)	1.29 (0.84)	0.23 ^d	<0.001 ^d
WMH pathology (–/+)	16/14	14/13			0.91 ^e	

^aDefined as WMH volume \geq 0.5% of total intracranial volume (ICV).

^bunavailable for 9 participants.

^cderived from FLAIR segmentation, available for 24 PiB–, 26 PiB+, 28 WMH–, 22 WMH+.

^dp-value from MANOVA, df = 1,55.

^ep-value from Pearson Chi-Square test.

doi:10.1371/journal.pone.0065175.t001

the one subject with 2/4 apoE genotype was not included in the apoE ϵ 4 positive group.

WMH Pathology

WMH were segmented from skull-stripped, intensity inhomogeneity corrected FLAIR images [31,32]. The WMH lesion segmentations were visually inspected to ensure that the segmentations included at least 80% of observed WMH. This labor intensive process was only performed on participants with WMH lesions that appeared on 3 consecutive slices in all 3 orientations (50 of the 57 participants). Participants who did not meet this criterion were classified as not having WMH pathology. WMH pathology was operationalized as WMH volume greater than 0.5% of TIV (28 of the 57 participants).

DTI Processing

Preprocessing of the DTI data involved skull-stripping, motion and eddy-current correction with FSL package, geometric distortion correction [33]. After the creation of FA images for each participant, an automated region of interest (ROI) extraction was performed. First, all FA images were resliced to the SPM8 white matter (WM) template using a rigid-body transformation (dimensions: 121 \times 145 \times 121 voxels, resolution: 1.5 mm³). Next, the 'JHU ICBM-DTI-81' atlas package [34], which includes a probabilistic FA atlas and anatomical labels of 50 deep WM ROIs from the DTI data of 81 subjects, was imported into SPM8, co-registered, and resliced to the SPM8 WM template. Next, the resliced FA images were normalized to an intensity-averaged FA template generated from 23 Aging Brain research participants (mean age 75 \pm 6; 8 female) who had no infarcts and whose WMH burden volume was less than 0.5% of intracranial volume (ICV), considered significant WMH pathology [11], using a diffeomorphic registration algorithm (DARTEL) [35]. Finally, the individual FA images and the 'JHU ICBM-DTI-81' FA atlas were warped to the common space of the averaged FA template generated from 23 VBI- participants, whose DTI data, other than use in creation of the intensity-averaged FA template, were not

part of the current analyses. To avoid inclusion of surrounding gray matter or cerebral spinal fluid, DTI values were obtained only in voxels where FA was greater than 0.20.

Based on the literature and a priori hypotheses, FA were extracted from 9 tracts of interest that included the corona radiata and internal capsule (projection fibers), cingulum gyrus and parahippocampal white matter, and fornix (limbic fibers), superior longitudinal fasciculus, inferior and superior fronto-occipital fasciculi (association fibers), and corpus callosum. Figure 1 shows examples of the a priori tracts of interest overlaid on the intensity-averaged FA template.

PET: Acquisition

PiB-PET imaging was conducted at Lawrence Berkeley National Laboratory using a Siemens ECAT EXACT HR PET scanner in 3D acquisition mode. The PiB radiotracer was synthesized using a previously published protocol [36] and 10–15 mCi of PiB was injected as a bolus into an antecubital vein. Dynamic acquisition frames (34 or 35 frames total) were obtained over 90 minutes as following: 4 \times 15 seconds, 8 \times 30 seconds, 9 \times 60 seconds, 2 \times 180 seconds, 8 \times 300 or 10 \times 300 seconds, and 3 \times 600 or 2 \times 600 seconds. For additional details see [37].

PET: Processing and Analysis

PiB-PET data was preprocessed using the Statistical Parametric Mapping software package (SPM8; <http://www.fil.ion.ucl.ac.uk/spm>). Region of Interest (ROI) labeling, including the cerebellum gray matter masked, was implemented using the FreeSurfer v5.1 software package (<http://surfer.nmr.mgh.harvard.edu/>). Distribution volume ratio (DVR) images were created using Logan graphical analysis with PiB frames corresponding to 35–90 minutes post-injection and a gray matter cerebellar mask as the reference region [38,39]. The grey matter cerebellum was chosen as the reference region because it is known to be relatively unaffected by fibrillar amyloid in AD and is thus valuable to estimate non-specific PiB binding [39,40].

Table 2. Description of infarcts in 22 participants.

Number of Infarcts	N
1 infarct	16
2 infarcts	5
4 infarcts	1
Infarct size	
Small (3–10 mm)	17
Large (>10 mm)	13
Infarct severity	
Cystic	22
Not cystic	8
Vascular territory affected	
Middle cerebral artery	15
Anterior cerebral artery	2
Posterior cerebral artery	3
Basilar artery	6
Posterior inferior cerebellar artery	4
Hemisphere affected	
Right	18
Left	12
Infarct location	
Frontal gray matter	6
Frontal white matter	7
Parietal gray matter	4
Parietal white matter	4
Temporal white matter	1
Subcortical gray matter ¹	13
Corpus callosum or internal capsule	4
Other ²	11

¹basal ganglia and/or thalamus.

²midbrain, pons, medulla and/or cerebellum.

doi:10.1371/journal.pone.0065175.t002

ROIs were defined in each subject's native space using the Desikan-Killiany atlas and the semi-automated FreeSurfer processing stream [41]. A global measure of PiB uptake (Global PiB Index) was derived by averaging the mean DVR value from frontal (cortical regions anterior to the precentral gyrus), temporal (middle and superior temporal regions), parietal (supramarginal gyrus, inferior/superior parietal lobules and precuneus) and anterior and posterior cingulate ROIs. ROIs that overlapped with large cortical infarcts or cerebellar cortical infarcts were manually edited so that DVR values excluded these regions.

Subjects were classified as having high or low PiB uptake using a previously described cutoff approach [37]. That is, subjects were classified PiB positive if their global PiB uptake was 2 SD above (i.e., >1.08) of the mean PiB index value of 11 young subjects (age range = 20–30) unlikely to have amyloid deposition.

Statistical Analyses

All analyses were conducted using IBM SPSS Statistics software (version 20.0). Associations among dichotomous variables were assessed using Pearson Chi-Square test. We used multivariate analysis of covariance (MANCOVA) to evaluate the effects of WMH pathology and PiB status on FA from the 9 a priori tracts of interest, controlling for age, CDR, and presence of infarct.

Because we had no a priori hypotheses about laterality, FA from homologous parcels was averaged across hemispheres to reduce the number of comparisons. To further protect against type I error, we combined several of the 'JHU ICBM-DTI-81' white matter parcels (i.e., anterior, superior, and posterior regions of the corona radiata, anterior, posterior, and retrolenticular sections of the internal capsule, and 4 subregions of the cingulate gyrus). We examined the 3 subregions of the corpus callosum (i.e., genu, body, and splenium) separately because we wanted to test the patho-anatomic model for regional disruption of callosal FA proposed by Lee et al [27]. In secondary analyses, we re-evaluated the effects of WMH pathology and PiB status on FA from the 9 a priori tracts of interest in the subset of subjects who had no infarct(s) and controlled for the effects of apoE ε4 in the subset of subjects who had apoE genotype information.

Results

Participant Characteristics

Table 1 summarizes the demographic and clinical data of participants by PiB and WMH pathology status. There were no significant differences in age, sex, education, Mini-Mental State Examination (MMSE), Geriatric Depression Scale (GDS) scores, WMH volume, apoE ε4 status, or frequency of brain infarct among PiB negative (N = 30) and positive (N = 27) participants. However, more PiB positive subjects had CDR score of 0.5 ($\chi^2 = 3.93$, $df = 1$, $p < 0.05$) than PiB negative. There were no significant age, sex, education, MMSE, GDS, CDR, apoE, global PiB index, or frequency of brain infarct among participants with (N = 27) or without (N = 30) WMH pathology. As expected, WMH volume was larger among participants with than without WMH pathology ($F_{1,48} = 46.09$, $p = 0.001$). Twenty-two participants (3 WMH–PiB–; 6 WMH+PiB–; 7 WMH– PiB+; 6 WMH+PiB+) had radiologic evidence infarct(s). A summary of the description of the participants' infarcts is presented in Table 2.

Table 3 summarizes the effects of PiB positivity and WMH pathology on FA values from the 9 tracts of interest by group. After controlling for age, CDR, and presence of infarct(s), PiB positivity was associated with lower FA in the fornix ($F_{1,50} = 6.69$, $p = 0.01$) and the splenium of the corpus callosum ($F_{1,50} = 4.20$, $p < 0.05$). WMH pathology was associated with lower FA in the corona radiata ($F_{1,50} = 23.34$, $p < 0.001$), internal capsule ($F_{1,50} = 23.53$, $p < 0.001$), superior longitudinal fasciculus ($F_{1,50} = 12.72$, $p = 0.001$), superior fronto-occipital fasciculus ($F_{1,50} = 11.43$, $p = 0.001$), inferior fronto-occipital fasciculus ($F_{1,50} = 11.47$, $p = 0.001$), and body of the corpus callosum ($F_{1,50} = 7.9954$, $p = 0.01$). There was a positive interaction between PiB and WMH pathology in the internal capsule ($F_{1,50} = 6.39$, $p = 0.01$) and parahippocampal white matter ($F_{1,50} = 5.16$, $p = 0.03$), where PiB-related reductions in FA was greater among participants with WMH pathology.

Similar to the analysis in the entire study population, secondary analysis in the subset of subjects without infarct(s) revealed a marginal effect of PiB positivity on FA in the fornix ($F_{1,29} = 3.29$, $p = 0.08$) after controlling for age and CDR. WMH pathology was associated with lower FA in the corona radiata ($F_{1,29} = 21.67$, $p < 0.001$), internal capsule ($F_{1,29} = 14.56$, $p = 0.001$), superior longitudinal fasciculus ($F_{1,29} = 5.14$, $p = 0.03$), and inferior fronto-occipital fasciculus ($F_{1,29} = 5.38$, $p = 0.03$), and marginally lower FA in the superior fronto-occipital fasciculus ($F_{1,29} = 3.97$, $p = 0.06$) and body of the corpus callosum ($F_{1,29} = 3.89$, $p = 0.06$). There was a positive interaction between PiB and WMH pathology on FA in the internal capsule ($F_{1,29} = 4.24$, $p < 0.05$).

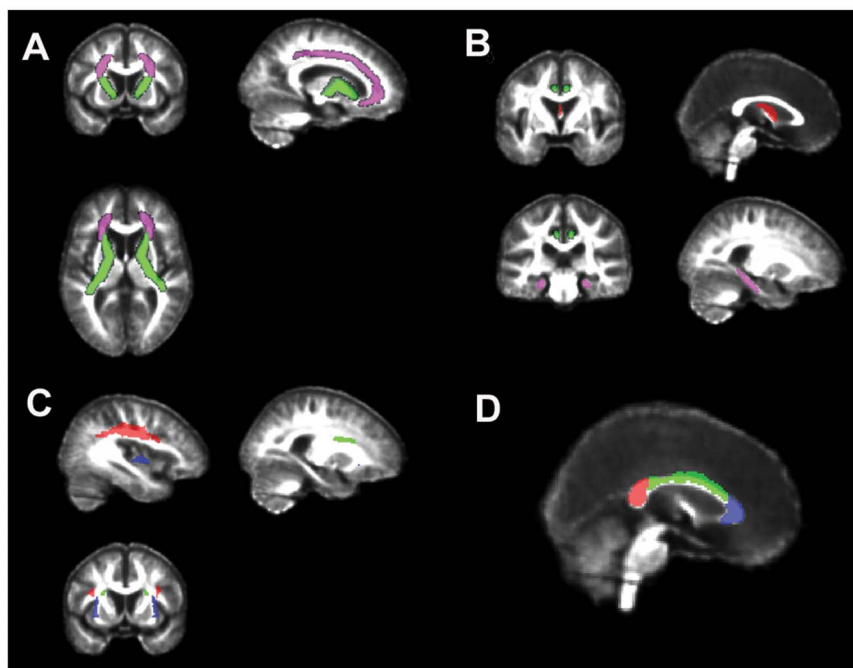


Figure 1. Examples of the (A) projection fiber ROIs: corona radiata in magenta; internal capsule in green, (B) limbic fiber ROIs: cingulate gyrus in green, parahippocampal white matter in magenta; fornix in red, (C) association fiber ROIs: superior longitudinal fasciculus in red; superior fronto-occipital fasciculus in green; inferior fronto-occipital fasciculus in purple, and (D) corpus callosum ROIs: genu in purple; body in green; splenium in red. ROIs are overlaid an intensity-averaged FA template generated from 23 Aging Brain research participants with no infarct and WMH <0.5% intracranial volume.
doi:10.1371/journal.pone.0065175.g001

and a marginally significant interaction in the parahippocampal white matter ($F_{1,29} = 3.97$, $p = 0.06$).

Table 4 summarizes results of the secondary analysis that accounted for apoE genotype. Because apoE genotyping was not

available for all subjects, we first examined the effects of PiB status and WMH pathology in the subset of subjects with apoE genotype, controlling age, CDR, and presence of infarct(s). This revealed a main effect of PiB positivity on FA in the fornix ($F_{1,41} = 4.84$,

Table 3. Least Squares Means FA values from 9 ROIs by PiB and WMH pathology status^a.

	PiB-WMH-	PiB-WMH+	PiB+WMH+	PiB+WMH+	p-value		
	(n = 16)	(n = 14)	(n = 14)	(n = 13)	PiB	WMH	PiB X WMH
Projection Fibers							
Corona radiata	0.40 (0.03)	0.38 (0.03)	0.41 (0.03)	0.36 (0.03)	0.38	<0.001	0.08
Internal capsule	0.51 (0.03)	0.50 (0.03)	0.53 (0.03)	0.48 (0.03)	0.65	<0.001	0.01
Limbic Fibers							
Cingulum	0.33 (0.03)	0.34 (0.03)	0.33 (0.03)	0.33 (0.03)	0.61	0.29	0.73
Parahippocampal WM	0.34 (0.03)	0.36 (0.03)	0.35 (0.03)	0.33 (0.03)	0.44	0.65	0.03
Fornix	0.36 (0.06)	0.33 (0.06)	0.30 (0.06)	0.30 (0.06)	0.01	0.45	0.29
Association Fibers							
Superior longitudinal fasciculus	0.41 (0.03)	0.39 (0.03)	0.41 (0.03)	0.38 (0.03)	0.46	0.001	0.37
Superior fronto-occipital fasciculus	0.39 (0.04)	0.34 (0.04)	0.37 (0.05)	0.34 (0.05)	0.64	0.001	0.48
Inferior fronto-occipital fasciculus	0.34 (0.02)	0.33 (0.02)	0.35 (0.02)	0.32 (0.02)	0.86	0.001	0.10
Corpus Callosum							
Genu	0.44 (0.03)	0.43 (0.03)	0.42 (0.03)	0.42 (0.04)	0.16	0.73	0.45
Body	0.50 (0.04)	0.47 (0.04)	0.49 (0.04)	0.46 (0.04)	0.19	0.007	0.67
Splenium	0.54 (0.03)	0.53 (0.03)	0.53 (0.03)	0.51 (0.04)	0.046	0.19	0.58

^aLeast squares means of FA values in PiB +/- and WMH +/- groups controlling for age, CDR, and presence of infarct.

^ap-values from MANCOVA, $df = 1,50$.

doi:10.1371/journal.pone.0065175.t003

$p = 0.03$) and in the splenium of the corpus callosum ($F_{1,41} = 4.11$, $p < 0.05$); a main effect of WMH pathology on FA in the corona radiata ($F_{1,41} = 24.33$, $p < 0.001$), internal capsule ($F_{1,41} = 26.35$, $p < 0.001$), superior longitudinal fasciculus ($F_{1,41} = 13.76$, $p = 0.001$), superior fronto-occipital fasciculus ($F_{1,41} = 8.00$, $p = 0.007$), inferior fronto-occipital fasciculus ($F_{1,41} = 7.95$, $p = 0.007$), and body of the corpus callosum ($F_{1,41} = 6.49$, $p = 0.02$); and interactions between PiB and WMH pathology on FA in the internal capsule ($F_{1,41} = 4.10$, $p < 0.05$) and parahippocampal white matter ($F_{1,41} = 3.97$, $p = 0.05$). In a second MANCOVA that controlled for apoE $\epsilon 4$ status in addition to age, CDR, and presence of infarcts, there was a main effect of PiB on fornix ($F_{1,40} = 6.09$, $p = 0.02$) and splenium ($F_{1,40} = 5.23$, $p = 0.03$) FA and a main effect of WMH pathology on FA in the corona radiata ($F_{1,40} = 23.87$, $p < 0.001$), internal capsule ($F_{1,40} = 25.91$, $p < 0.001$), superior longitudinal fasciculus ($F_{1,40} = 13.51$, $p = 0.001$), superior fronto-occipital fasciculus ($F_{1,40} = 7.78$, $p = 0.008$), inferior fronto-occipital fasciculus ($F_{1,40} = 8.02$, $p = 0.007$), and body of the corpus callosum ($F_{1,40} = 6.65$, $p = 0.01$). However, the interaction between PiB and WMH pathology in the internal capsule ($F_{1,40} = 3.89$, $p = 0.06$) and parahippocampal white matter ($F_{1,40} = 3.91$, $p = 0.06$) were no longer significant.

Discussion

In our examination of the effects of WMH pathology and A β deposition on white matter microstructural integrity, we found that (1) WMH pathology was significantly associated with reduced FA in projection and association fibers. (2) A β deposition was significantly associated with reduced FA in the fornix and splenium of the corpus callosum. (3) Although there were positive interactions between WMH pathology and A β deposition on FA in the internal capsule and parahippocampal white matter, accounting for apoE genotype rendered these interactions only

marginally significant. Possible mechanisms and interpretations of the interaction are discussed below.

As hypothesized, WMH pathology was associated with reduced FA in projection and association fibers. This finding is consistent with earlier reports of an inverse relationship between FA and WMH volume [42], reduced FA in the presence of gliosis or infarcts [43,44], extending beyond normal appearing white matter in subjects with cerebral amyloid angiopathy [45], cerebral autosomal dominant arteriopathy with subcortical infarcts and leukoencephalopathy (CADASIL) [46], and cognitive impairment with and without vascular dementia [47]. These results are also in agreement with prior reports that ischemic brain disease [48,49] and vascular risk [15] alter FA in normal appearing white matter. The projection and association fiber tracts where we detected significant WMH pathology effects also correspond to the cerebral white matter regions with intermediate-high to low baseline anisotropy that Lee and colleagues [15] previously reported were most vulnerable to vascular risk.

As hypothesized, A β deposition was significantly associated with reduced FA in the fornix and splenium of the corpus callosum. Several studies have demonstrated that A β deposition can lead to DTI changes in mice [50,51]. One previous study examined DTI changes associated with cerebral spinal fluid (CSF) A β levels in humans and found that A $\beta 42$ levels were related to lower FA in medial frontal cortex and underlying white matter [52]. To the best of our knowledge, this is the first study to examine the relationship between cerebral A β deposition and FA. In the current study PiB positivity was associated with lower FA in the fornix, a predominant outflow tract of the hippocampus and a brain region affected early in the course of AD, consistent with previous DTI studies of MCI and AD [53–55]. PiB positivity was also associated with lower FA in the splenium of the corpus callosum, in accordance with previous ROI-based DTI studies of MCI and AD [56].

Table 4. Effects of PiB positivity and WMH pathology on FA in subset of subjects with apoE genotype^a.

	p-value from MANCOVA ^b			Controlling for apoE ^c		
	PIB effect	WMH effect	PIB X WMH	PIB effect	WMH effect	PIB X WMH
Projection Fibers						
Corona radiata	0.45	<0.001	0.33	0.42	<0.001	0.34
Internal capsule	0.79	<0.001	0.049	0.72	<0.001	0.06
Limbic Fibers						
Cingulum	0.96	0.45	0.86	0.90	0.46	0.88
Parahippocampal WM	0.62	0.77	0.05	0.66	0.77	0.06
Fornix	0.03	0.90	0.30	0.02	0.93	0.26
Association Fibers						
Superior longitudinal fasciculus	0.57	0.001	0.66	0.73	0.001	0.62
Superior fronto-occipital fasciculus	0.78	0.007	0.14	0.92	0.008	0.15
Inferior fronto-occipital fasciculus	0.66	0.007	0.30	0.81	0.007	0.33
Corpus Callosum						
Genu	0.39	0.62	0.57	0.31	0.61	0.54
Body	0.28	0.01	0.64	0.20	0.01	0.59
Splenium	0.049	0.16	0.36	0.03	0.15	0.40

^aPiB+WMH+: n = 13; PiB+WMH-: n = 14; PiB-WMH+: n = 14; PiB-WMH-: n = 16.

^bcontrolling for age, CDR, and presence of infarct, df = 1,41.

^cp-values from MANCOVA controlling for age, CDR, presence of infarct, and apoE $\epsilon 4$ status, df = 1,40.

doi:10.1371/journal.pone.0065175.t004

There is evidence suggesting that vascular brain injury exerts subtle deleterious effects on brain structure and function beyond frank infarction or hemorrhage [57–59]. For example, epidemiological studies have linked vascular risk factors (e.g., hypertension, hyperlipidemia, diabetes mellitus) to increased incidence of clinically-diagnosed AD [24,25]. Therefore, we hypothesized that there would be an interaction between WMH pathology and A β deposition on FA. In the current study, we found an interaction between WMH pathology and PiB positivity in the internal capsule and parahippocampal white matter, where PiB-related reductions in FA was greater among participants who also had WMH pathology. However, these interactions were no longer significant after controlling for apoE ϵ 4 genotype.

One possible mechanism by which WMH pathology and A β deposition might interact positively to degrade white matter microstructure is through the reduction of brain reserve. Reserve is the concept that there are characteristics of the brain that buffer the impact of pathology on brain performance [60,61]. The characteristics may be structural (e.g., ‘extra’ neurons and/or synapses) or functional (e.g., a degree of excess capacity or compensatory mechanisms such that the brain could continue to perform well despite damage [62]). There is suggestive evidence that WMHs have a negative effect on structural brain reserve. For example, a population-based study of 1,077 non-demented elderly (60–90 years old) individuals found that greater periventricular WMH severity was associated with a greater risk for developing dementia. Moreover, the association between WMH and dementia risk was independent of vascular risk factors, cerebral infarcts, and brain atrophy [63]. Hypertension, one of the strongest risk factor for WMHs, has also been linked with increased risk of developing AD [64] and treatment of hypertension has been found to be protective against the development of dementia [65]. Thus, in the context of the present study, it could be possible that WMH pathology was related to reduced structural brain reserve, which in turn rendered individuals with WMH pathology more vulnerable to the effects of cortical A β and AD pathology. Although it is not clear how precisely WMH pathology degrades brain reserve, some possible mechanisms include impaired neurogenesis and inflammation. Adult stem cells are located in the subventricular region [66], which is frequently affected by WMHs. Thus, the ischemic changes that lead to the development of WMHs could also cause damage to adult stem cells, impairing neurogenesis. Because there is microglial activation in brain tissue affected by WMHs [67] and

higher C-reactive protein levels in patients with WMHs [68], WMH pathology may also negatively impact reserve through inflammatory cytokines. It is noteworthy that the interaction between WMH pathology and PiB positivity were no longer significant after controlling for apoE ϵ 4 genotype. This suggests that another explanation for the interaction between WMH pathology and PiB may be apoE ϵ 4. Presence of the apoE ϵ 4 allele has been associated with increased amyloid deposition in the parenchyma [69] and amyloid positivity. Presence of the apoE ϵ 4 allele may also be associated with amyloid deposition in the blood vessels, which could be associated with CAA and WMH pathology [70]. Future studies with a longitudinal design will be needed to examine if increased amyloid deposition in each of these regions is in fact associated with decreased white matter microstructural integrity in different regions of the brain.

The current findings should be considered in the context of several study limitations: First, the study sample was the small and heterogeneous. Second, apoE genotyping was only available in a subset of subjects. Therefore, our interpretation of the role of apoE in the interaction between PiB positivity and WMH pathology on FA are speculative at best and should be regarded with caution. Other study limitations include the low angular resolution of DTI (6 directions), the fact that we did not account for the location of vascular lesions in our analyses of FA values obtained from 9 white matter tracts that covered most of the supratentorial white matter, and the cross-sectional nature of the study design. Future studies with a longitudinal design will be able to better resolve the nature of the relationship between WMH pathology and PiB positivity on white matter microstructural integrity in different regions of the brain.

Acknowledgments

We thank the staff at the Center for the Imaging of Neurodegenerative Diseases at the San Francisco VA and the imaging facilities at USC, UC Davis, and UCSF for help with data acquisition and preparation. We thank the recruiters of the Aging Brain Program Project.

Author Contributions

Conceived and designed the experiments: WJ CD HC MW. Performed the experiments: SK JL DT. Analyzed the data: LC SK DT JL YZ SV NS. Wrote the paper: LC CD MW SV HC WJM.

References

1. Neuropathology Group of the Medical Research Council Cognitive Function and Aging Study (MRC CFAS) (2001) Pathological correlates of late-onset dementia in a multicentre, community-based population in England and Wales. *Lancet* 357: 169–175.
2. Breteler MM, van Swieten JC, Bots ML, Grobbee DE, Claus JJ, et al. (1994) Cerebral white matter lesions, vascular risk factors, and cognitive function in a population-based study: the Rotterdam Study. *Neurology* 44: 1246–1252.
3. de Leeuw FE, de Groot JC, Oudkerk M, Witteman JC, Hofman A, et al. (200) Aortic atherosclerosis at middle age predicts cerebral white matter lesions in the elderly. *Stroke* 31: 425–429.
4. de Leeuw FE, de Groot JC, Oudkerk M, Witteman JC, Hofman A, et al. (2002) Hypertension and cerebral white matter lesions in a prospective cohort study. *Brain* 125: 765–772.
5. Chen YW, Gurol ME, Rosand J, Viswanathan A, Rakich SM, et al. (2006) Progression of white matter lesions and hemorrhages in cerebral amyloid angiopathy. *Neurology* 67: 83–87.
6. Hardy J, Selkoe DJ (2002) The amyloid hypothesis of Alzheimer’s disease: progress and problems on the road to therapeutics. *Science* 297: 353–356.
7. Schneider JA, Arvanitakis Z, Bang W, Bennett DA (2007) Mixed brain pathologies account for most dementia cases in community-dwelling older persons. *Neurology* 69: 2197–2204.
8. Lee JH, Kim SH, Kim GH, Seo SW, Park HK, et al. (2011) Identification of pure subcortical vascular dementia using 11C-Pittsburgh compound B. *Neurology* 77: 18–25.
9. Reed BR, Marchant NL, Jagust WJ, DeCarli CC, Mack W, et al. (2012) Coronary risk correlates with cerebral amyloid deposition. *Neurobiol Aging* 33: 1979–1987.
10. Chui HC, Zarow C, Mack WJ, Ellis WG, Zheng L, et al. (2006) Cognitive impact of subcortical vascular and Alzheimer’s disease pathology. *Ann Neurol* 60: 677–687.
11. DeCarli C, Murphy DG, Tranh M, Gracy CL, Haxby JV, et al. (1995) The effect of white matter hyperintensity volume on brain structure, cognitive performance, and cerebral metabolism of glucose in 51 healthy adults. *Neurology* 45: 2077–2084.
12. Basser PJ, Mattiello J, LeBihan D (1994) Estimation of the effective self-diffusion tensor from the NMR spin echo. *J Magn Reson B* 103: 247–254.
13. Beaulieu C (2002) The basis of anisotropic water diffusion in the nervous system – a technical review. *NMR Biomed* 15: 435–455.
14. Werring DJ, Toosy AT, Clark CA, Parker GJ, Barker GJ, et al. (2000) Diffusion tensor imaging can detect and quantify corticospinal tract degeneration after stroke. *J Neurol Neurosurg Psychiatry* 69: 269–272.
15. Lee DY, Fletcher E, Martinez O, Ortega M, Zozulya N, et al. (2009) Regional pattern of white matter microstructural changes in normal aging, MCI, and AD. *Neurology* 73: 1722–1728.
16. Choo IH, Lee DY, Oh JS, Lee JS, Lee DS, et al. (2010) Posterior cingulate cortex atrophy and regional cingulum disruption in mild cognitive impairment and Alzheimer’s disease. *Neurobiol Aging* 31: 772–779.

17. Sexton CE, Kalu UG, Filippini N, Mackay CE, Ebmeier KP (2011) A meta-analysis of diffusion tensor imaging in mild cognitive impairment and Alzheimer's disease. *Neurobiol Aging* 32: 2322.e2325–2318.
18. Chua TC, Wen W, Chen X, Kochan N, Slavin MJ, et al. (2009) Diffusion tensor imaging of the posterior cingulate is a useful biomarker of mild cognitive impairment. *Am J Geriatr Psychiatry* 17: 602–613.
19. Zhang Y, Schuff N, Jahng GH, Bayne W, Mori S, et al. (2007) Diffusion tensor imaging of cingulum fibers in mild cognitive impairment and Alzheimer disease. *Neurology* 68: 13–19.
20. Fellgiebel A, Müller MJ, Wille P, Dellani PR, et al. (2005) Color-coded diffusion-tensor-imaging of posterior cingulate fiber tracts in mild cognitive impairment. *Neurobiol Aging* 26: 1193–1198.
21. Delano-Wood L, Bondi MW, Jak AJ, Horne NH, Schweinsburg BC, et al. (2010) Stroke risk modifies regional white matter differences in mild cognitive impairment. *Neurobiol Aging* 31: 1721–1731.
22. Utkar M, Makuc E, Onor ML, Garbin G, Trevisiol M, et al. (2008) Evaluation of white matter damage in patients with Alzheimer's disease and in patients with mild cognitive impairment by using diffusion tensor imaging. *Radiol Med* 113: 915–922.
23. Munoz DG, Hastak SM, Harper B, Lee D, Hachinski VC (1993) Pathologic correlates of increased signals of the centrum ovale on magnetic resonance imaging. *Arch Neurol* 50: 492–497.
24. Reitz C, Tang MX, Schupf N, Manly JJ, Mayeux R, et al. (2010) A summary risk score for the prediction of Alzheimer disease in elderly persons. *Arch Neurol* 67: 835–841.
25. Qiu C, Xu W, Winblad B, Fratiglioni L (2010) Vascular risk profiles for dementia and Alzheimer's disease in very old people: a population-based longitudinal study. *J Alzheimer's Dis* 20: 293–300.
26. Viswanathan A, Rocca WA, Tzourio C (2009) Vascular risk factors and dementia: how to move forward? *Neurology* 72: 368–374.
27. Lee DY, Fletcher E, Martinez O, Zozulya N, Kim J, et al. (2010) Vascular and degenerative processes differentially affect regional interhemispheric connections in normal aging, mild cognitive impairment, and Alzheimer disease. *Stroke* 41: 1797–1797.
28. Morris JC (1993) The Clinical Dementia Rating (CDR): Current version and scoring rules. *Neurology* 43: 2412–2414.
29. Griswold MA, Jakob PM, Heidemann RM, Heidemann RM, Nittka M, et al. (2002) Generalized autocalibrating partially parallel acquisitions (GRAPPA). *Magn. Reson. Med* 47: 1202–1210.
30. Corder EH, Saunders AM, Risch NJ, Strittmatter WJ, Schmechel DE, et al. (1994) Protective effect of apolipoprotein e type 2 allele for late onset alzheimer disease. *Nat Genet* 7: 180–184.
31. Hadjimetriou S, Studholme C, Mueller S, Weiner M, Schuff N (2009) Restoration of MRI data for intensity non-uniformities using local high order intensity statistics. *Med Image Anal* 13: 36–48.
32. Hadjimetriou S, Lorenzen P, Schuff N, Mueller S, Weiner M (2008) Computational atlases of severity of white matter lesions in elderly subjects with MRI. *Med Image Comput Comput Interv* 11: 450–458.
33. Tao R, Fletcher PT, Gerber S, Whitaker RA (2009) A variational image-based approach to the correction of susceptibility artifacts in the alignment of diffusion weighted and structural MRI. *Inf Process Med Imaging* 21: 651–663.
34. Oishi K, Zilles K, Amunts K, Faria A, Jiang H, et al. (2008) Human brain white matter atlas: identification and assignment of common anatomical structures in superficial white matter. *Neuroimage* 43: 447–457.
35. Ashburner J (2007) A fast diffeomorphic image registration algorithm. *Neuroimage* 38: 95–113.
36. Mathis CA, Wang Y, Holt DP, Huang GF, Debnath ML, et al. (2003) Synthesis and evaluation of 11C-labeled 6-substituted 2-arylbenzothiazoles as amyloid imaging agents. *J Med Chem* 46: 2740–2754.
37. Mormino EC, Brandel MG, Madison CM, Rabinovici GD, Marks S, et al. (2012) Not quite PIB-positive, not quite PIB-negative: Slight PIB elevations in elderly normal control subjects are biologically relevant. *Neuroimage* 59: 1152–1160.
38. Logan J, Fowler JS, Volkow ND, Wang GJ, Ding YS, et al. (1996) Distribution volume ratios without blood sampling from graphical analysis of PET data. *J Cereb Blood Flow Metab* 16: 834–840.
39. Price JC, Klunk WE, Lopresti BJ, Lu X, Hodge JA, et al. (2005) Kinetic modeling of amyloid binding in humans using PET imaging and Pittsburgh Compound-B. *J Cereb Blood Flow Metab* 25: 1528–1547.
40. Klunk WE, Engler H, Nordberg A, Wang Y, Blomqvist G, et al. (2004) Imaging brain amyloid in Alzheimer's disease with Pittsburgh Compound-B. *Ann Neurol* 55: 306–319.
41. Desikan RS, Segonne F, Fischl B, Quinn BT, Dickerson BC, et al. (2006) An automated labeling system for subdividing the human cerebral cortex on MRI scans into gyral based regions of interest. *Neuroimage* 31: 968–980.
42. Zhan W, Zhang Y, Mueller SG, Lorenzen P, Hadjimetriou S, et al. (2009) Characterization of white matter degeneration in elderly subjects by magnetic resonance diffusion and FLAIR imaging correlation. *Neuroimage (Suppl 2)*: T58–65.
43. Buffon F, Molko N, Herve D, Porcher R, Denghien I, et al. (2005) Longitudinal diffusion changes in cerebral hemispheres after MCA infarcts. *J Cereb Blood Flow Metab* 25: 641–650.
44. Gupta RK, Saksena S, Hasan KM, Agarwal A, Haris M, et al. (2006) Focal Wallerian degeneration of the corpus callosum in large middle cerebral artery stroke: serial diffusion tensor imaging. *J Magn Reson Imaging* 24: 549–555.
45. Salat DH, Smith EE, Tuch DS, Benner T, Pappu V, et al. (2006) White matter alterations in cerebral amyloid angiopathy measured by diffusion tensor imaging. *Stroke* 37: 1759–1764.
46. Chhabriat H, Pappata S, Poupon C, Clark CA, Vahedi K, et al. (1999) Clinical severity in CADASIL related to ultrastructural damage in white matter: in vivo study with diffusion tensor MRI. *Stroke* 30: 2637–2643.
47. Xu Q, Zhou Y, Li YS, Cao WW, Lin Y, et al. (2010) Diffusion tensor imaging changes correlate with cognition better than conventional MRI findings in patients with subcortical ischemic vascular disease. *Dement Geriatr Cogn Disord* 30: 317–326.
48. O'Sullivan M, Summers PE, Jones DK, Jarosz JM, Williams SCR, et al. (2001) Normal-appearing WM in ischemic leukoariosis: a diffusion tensor MRI study. *Neurology* 57: 2307–2310.
49. O'Sullivan M, Morris RG, Huckstep B, Jones DK, Williams SC, et al. (2004) Diffusion tensor MRI correlates with executive dysfunction in patients with ischaemic leukoariosis. *J Neurol Neurosurg Psychiatry* 75: 441–447.
50. Song SK, Kim JH, Lin SJ, Brendza RP, Holtzman DM (2004) Diffusion tensor imaging detects age-dependent white matter changes in a transgenic mouse model with amyloid deposition. *Neurobiol Dis* 15: 640–647.
51. Sun SW, Song SK, Harms MP, Lin SJ, Holtzman DM, et al. (2005) Detection of age-dependent brain injury in a mouse model of brain amyloidosis associated with Alzheimer's disease using magnetic resonance diffusion tensor imaging. *Exp Neurol* 191: 77–85.
52. Bendlin BB, Carlsson CM, Johnson SC, Zetterberg H, Blennow K, et al. (2012) CSF T-Tau/A β 42 predicts white matter microstructure in healthy adults at risk for Alzheimer's disease. *PLoS One* 7: e37720.
53. Mielke MM, Kozauer NA, Chan KC, Cheorge M, Toroney J, et al. (2009) Regionally-specific diffusion tensor imaging in mild cognitive impairment and Alzheimer's disease. *Neuroimage* 46: 47–55.
54. Mielke MM, Okonkwo OC, Oishi K, Mori S, Tighe S, et al. (2012) Fornix integrity and hippocampal volume predict memory decline and progression to Alzheimer's disease. *Alzheimers Dement* 8: 105–113.
55. Nowrangi MA, Lyketsos CG, Leoutsakos JM, Oishi K, Albert M, et al. (2012) Longitudinal, region-specific course of diffusion tensor imaging measures in mild cognitive impairment and Alzheimer's disease. *Alzheimers Dement* [Epub Dec 12, 2012].
56. Chua TC, Wen W, Slavin MJ, Sachdev PS (2008) Diffusion tensor imaging in mild cognitive impairment and Alzheimer's disease: a review. *Curr Opin Neurol* 21: 83–92.
57. Mungas D, Jagust WJ, Reed BR, Kramer JH, Weiner MW, et al. (2001) MRI predictors of cognition in subcortical ischemic vascular disease and Alzheimer's disease. *Neurology* 57: 2229–2235.
58. Mungas D, Harvey D, Reed BR, Jagust WJ, DeCarli C, et al. (2005) Longitudinal volumetric MRI change and rate of cognitive decline. *Neurology* 65: 565–571.
59. Jagust WJ, Zheng L, Harvey DJ, Mack WJ, Vinters HV, et al. (2008) Neuroanatomical basis of magnetic resonance images in aging and dementia. *Ann Neurol* 63: 72–80.
60. Satz P (1993) Brain reserve capacity on symptom onset after brain injury: formulation and review of evidence for threshold theory. *Neuropsychology* 7: 273–295.
61. Stern Y (2002) What is cognitive reserve? Theory and research application of the reserve concept. *J Int Neuropsychol Soc* 8: 448–460.
62. Stern Y (2009) Cognitive reserve. *Neuropsychologia* 47: 2015–2028.
63. Prins ND, van Dijk EJ, den Heijer T, Vermeer SE, Koudstaal PJ, et al. (2004) Cerebral white matter lesions and the risk of dementia. *Arch Neurol* 61: 1531–1534.
64. Prince M, Cullen M, Mann A (1994) Risk factors for Alzheimer's disease and dementia: a case-control study based on the MRC elderly hypertension trial. *Neurology* 44: 97–104.
65. Forette F, Seux ML, Staessen JA, Thijs L, Babarskiene MR, et al. (2002) Systolic Hypertension in Europe Investigators. The prevention of dementia with antihypertensive treatment: new evidence from the Systolic Hypertension in Europe (Syst-Eur) study. *Arch Intern Med* 162: 2046–2052.
66. Picard-Riera N, Nait-Oumesmar B, Baron-Van Evercooren A (2004) Endogenous adult neural stem cells: limits and potential to repair the injured central nervous system. *J Neurosci Res* 76: 223–231.
67. Fernando MS, Simpson JE, Matthews F, Brayne C, Lewis CE, et al. (2006) White matter lesions in an unselected cohort of the elderly: molecular pathology suggests origin from chronic hypoperfusion injury. *Stroke* 37: 1391–1398.
68. van Dijk EJ, Prins ND, Vermeer SE, Vrooman HA, Hofman A, et al. (2005) C-reactive protein and cerebral small-vessel disease: the Rotterdam Scan Study. *Circulation* 112: 900–905.
69. Ramanan VK, Risacher SL, Nho K, Kim S, Swaminathan S, et al. (2013) APOE and BCHE as modulators of cerebral amyloid deposition: a florbetapir PET genome-wide association study. *Mol Psychiatry* [Epub Feb 19, 2013].
70. Gurol ME, Viswanathan A, Gidicsin C, Hedden T, Martinez-Ramirez S, et al. (2012) Cerebral amyloid angiopathy burden associated with leukoariosis: A positron emission tomography/magnetic resonance imaging study. *Ann Neurol* [Epub Dec. 13, 2012].